System for the Measurement of Spectral Emittance at High Temperature

James O. Hylton*
Tennessee Valley Authority, Knoxville, Tenn.
and
Robert L. Reid†
Cleveland State University, Cleveland, Ohio

A system for measuring the emittance of refractory materials in vacuum for temperatures up to 3000°C in the wavelength range of 0.4–5.0 has been developed and tested. In preferred operation, the specimen is machined to contain its own reference cavity. An optical nulling measurement system was developed in which the radiation from the sample and a reference lamp are focused alternately on the entrance aperture of a monochromator. Detailed error analysis and comparison with literature data for tungsten showed the system to be accurate to ±0.02 for emittances above 0.50. Graphite, carbon foam, and aluminum oxide also were measured.

Introduction

THE reflection of electromagnetic radiation from real surfaces has been studied extensively, both experimentally and theoretically. The emittance and reflectance of certain types of surfaces can be predicted from classical electromagnetic theory. Much experimental work has been done in order to verify theoretical predictions and to provide data for engineering applications.

Many industrial applications have led to the need for accurate data on the spectral emittance of various materials. One of the earliest was the use of refractory metals as filaments for incandescent lamps. Another was the widespread use of thermal radiation pyrometers to monitor and control industrial processes.

In the aerospace industry, heat transfer by radiation is a predominant factor in space vehicles. This has prompted a great deal of investigation into the emissive and reflective properties of many materials. The increasing interest in the collection of solar energy at high temperatures also will require similar data. High-temperature vacuum-type insulations are another application where thermal radiation properties must be known at elevated temperatures.

Gubareff[1] and Touloukian[2] have compiled much of the available radiation property data on a wide range of materials. Many different experimental techniques for measuring emittance have been developed and are described in the literature. Blau and Fischer[3] and Thorn and Winslow[4] have reviewed the work of several investigators and present some of the measurement methods which have evolved. In spite of the availability of a great deal of property data in the literature, it still is difficult to match required conditions in many cases. The system described here is the result of an effort to construct a general purpose emissometer for operation at temperatures up to 3000°C and at wavelengths from 0.4 to 5.0μ.

Presented as Paper 74-672 at the AIAA/ASME, 1974 Thermophysics and Heat Transfer Conference, Boston, Mass., July 15–17, 1974; submitted March 26, 1976; revision received May 3, 1976. This work was performed at Union Carbide Nuclear Division, Oak Ridge, Tenn. Further details are found in AEC Report Y-1914, Aug. 6, 1973, available NTIS.

Index categories: Liquid and Solid Thermophysical Properties; Radiation and Radiative Heat Transfer; Thermal Surface Properties.

*Mechanical Engineer (Instrumentation), Division of Engineering Design.

†Associate Professor, Mechanical Engineering Department.

Description of Equipment

The system was designed around two major components, which were already available (a high-temperature vacuum furnace and a ¼-m. Ebert Mount monochromator) and it includes many of the features described in the literature which are considered necessary to obtain good measurements at high temperatures. A cylindrical cavity machined into the sample material serves as the reference blackbody. An optical system and an energy detector were constructed to operate with the monochromator. Energy measurements are accomplished by comparing the intensity of radiation from the sample to the intensity of an internal reference lamp, which is adjusted until it matches the sample intensity. This principle has been used successfully in optical pyrometers for many years. The main advantage of this method is that it greatly simplifies the electronics required for the energy detector. Since the system calibration is determined by the intensity of the reference lamp, the energy detector and its associated electronics serve only as a null detector. Sources of error associated with amplifier gain, stability, linearity, and drift are significantly reduced. The reference lamp intensity is a stable function of its filament current, which can be supplied by a battery and adequately measured with a resistance bridge and galvanometer.

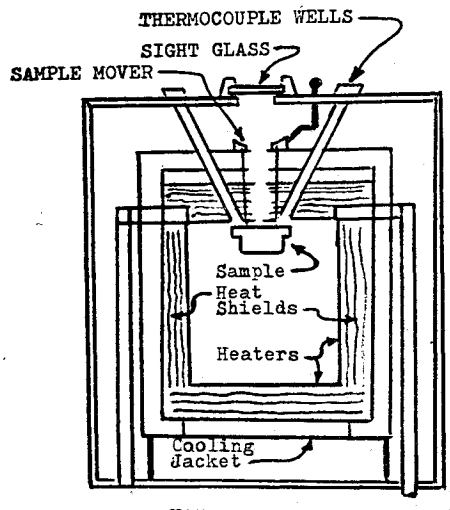

Fig. 1 Vacuum furnace details.

Vacuum Furnace

The source of heat must be able to heat the sample and reference cavity uniformly to the desired temperature and control it at that point until measurements are made. The heating should take place in a vacuum or an inert atmosphere in order to avoid contamination of the sample. Direct electrical or inductive heating generally is used whenever possible because it is easier to reach high temperatures and avoid temperature gradients. Radiant heating in a furnace offers greater flexibility in sample configurations and is not limited to materials that are conductors or susceptors. It is more difficult, however, to achieve uniform temperatures throughout the sample. Radiant heating was used here because some of the samples to be tested were neither electrical conductors nor magnetic susceptors.

The vacuum furnace is an ABAR Series 90, with tungsten electrodes. Figure 1 shows the internal details of the furnace. The heaters form a box-like hot zone approximately 4 in. square and 5 in. deep. The furnace can operate with hot zone temperatures up to 3000°C at pressures of 1×10^{-5} torr.

Spectrometer

Several types of optical pyrometers measure the radiant intensity of a source by superimposing the image of the source onto the filament of an internal lamp. The filament current is adjusted until the intensity of the filament matches the intensity of the source image. The relationship between the filament current and the source intensity has proven to be very stable over long periods of operation. Because of the proven reliability of this method in optical pyrometry, it was decided to build a spectrometer based on this principle.

A diagram of the spectrometer optical system is shown in Fig. 2. Light from the sample enters the sytem through an adjustable aperture at A. It passes through the chopper C and is focused by mirrors M2, M3, and M4 onto the entrance aperture E of a monochromator. The monochromator disperses the beam by means of a diffraction grating, and focuses the desired wavelength band onto the detector. The chopper C is cut from a front surface optical mirror and is positioned such that when a blade is blocking light from the sample, it is reflecting light from the reference lamp along the same path to the monochromator. Mirror M1 is adjusted so that the virtual image of the lamp formed by the chopper rotates, the beams from the sample and the lamp are focused alternately onto the monochromator entrance. The intensities of the two beams are compared by a detector at the monochromator exit.

Detector and Amplifier

Figure 3 illustrates the operation of the basic detector and amplifier circuit. The detector shown is photconductive lead sulfide, which has a sensitive response between wavelengths of 0.6 μ and approximately 2.5 μ. The detector bias is supplied by a 45-V radio battery. The detector output is a transformer coupled into a GR 1232A amplifier. The GR-1232A is a small transistorized amplifier with an adjustable filter and an output meter. The chopper, driven by a synchronous motor, switches the sample and reference beams at a rate of 100 Hz. This produces an ac signal, whose amplitude is proportional to the difference in intensity of the sample and the reference lamp. The sample intensity is measured by setting the amplifier gain at a high level and by adjusting the reference lamp current until the output meter is at a minimum.

It is in the relative simplicity of the detection circuitry that optical nulling offers an advantage. The only requirement is that the noise level be low enough that the "null" point can be established with the desired precision. In this regard, the alignment and surface quality of the optical components, especially the chopper, are critical. Once this is accomplished and the reference lamp is properly calibrated, any desired type of detector can be used. At visible wavelengths, the null point can be established fairly well by visual observation of the

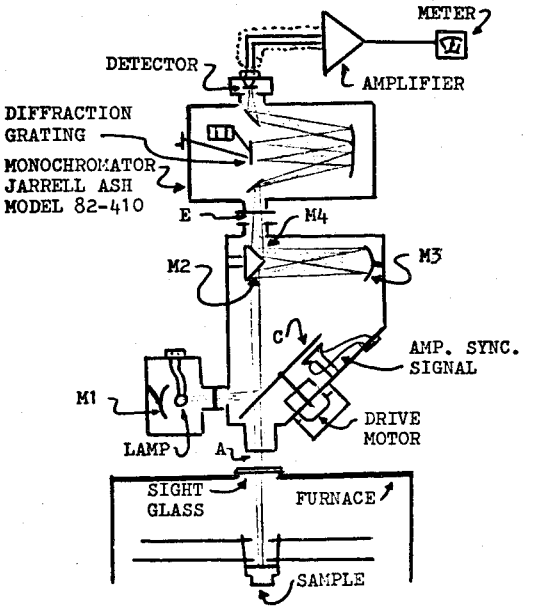

Fig. 2 Optical system.

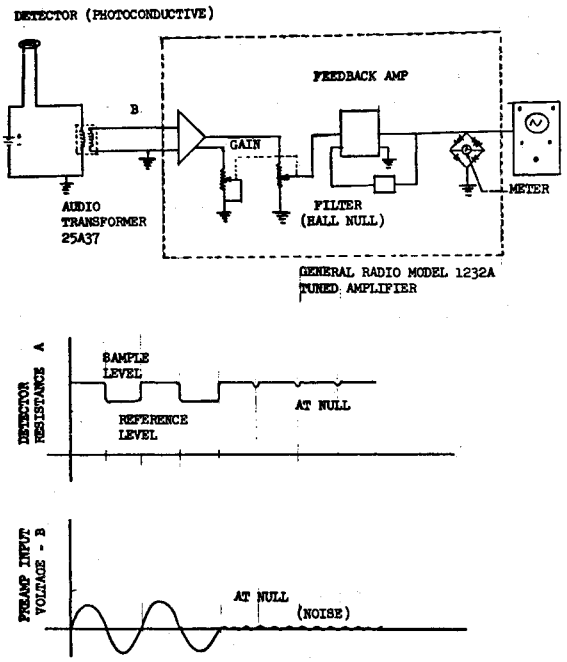

Fig. 3 Detector bias and amplifier circuit.

images. The circuit shown in Fig. 3 could determine the null point to within 1% of the overall sample intensity.

A 6-V dc bulb (a GE-1630) was used as the reference lamp. This lamp was found to be satisfactory for operation at wavelengths less than 3μ. The optical system was designed so that the reference lamp chamber could be evacuated and the glass envelope of the bulb could be removed to eliminate infrared absorption. This, however, was not necessary at the previously mentioned wavelengths. The lamp current (1-2A) was supplied by a battery or a small dc power supply, and was measured with a shunt and millivolt potentiometer.

The system was calibrated by inserting a series of neutral density filters (sector disks) into the sample beam and determining the null point corresponding to each filter. Figure 4 shows a typical calibration curve. The ordinate represents transmittance factors of the filters and the abcissa represents null current. A similar curve must be determined for each wavelength of interest. In operation, the null currents for two

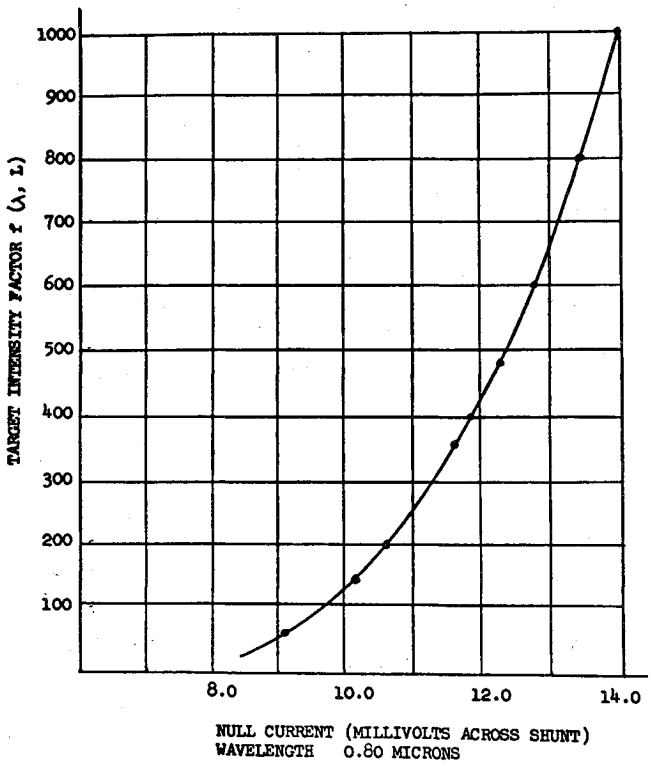

Fig. 4 Typical reference lamp calibration curve.

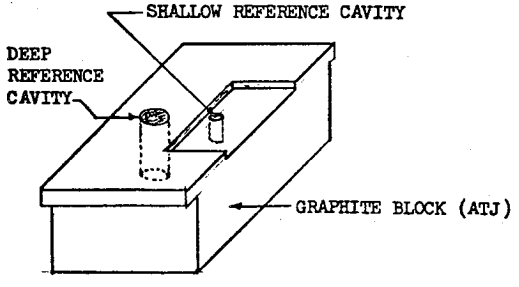

Fig. 5 Sample and reference cavity.

unknown sources are measured. The ratio of the intensity factors corresponding to the null currents will be the ratio of the intensities of the two sources.

Sample Block

The sample in Fig. 1 is shown suspended in the hot zone near the top shields. Figure 5 shows the configuration of the sample block. The reference blackbody is a cylindrical cavity drilled in the sample block. The sample block is supported by a mechanism that can be moved from outside the furnace to permit viewing of either the sample surface or the reference cavity. Because the sample block is receiving heat from the bottom and the sides of the hot zone, but not from the top, most of the heat transfer in the block is upward, toward the unheated top shields. It was found that the temperature gradient in the block would have a significant effect upon the emittance measurements and the evaluation of the reference cavity emittance. It was necessary to measure the temperature gradient accurately and correct for its effects. A shallow reference cavity was added for this purpose, as shown in Fig. 5.

In cases in which the sample material could not be formed into a block, the reference cavity was drilled into a graphite block. A sheet of the sample material was attached to the top of the block, as shown in Fig. 6. This however, added an additional problem because of a temperature drop across the contact resistance of the graphite-sample interface. In order

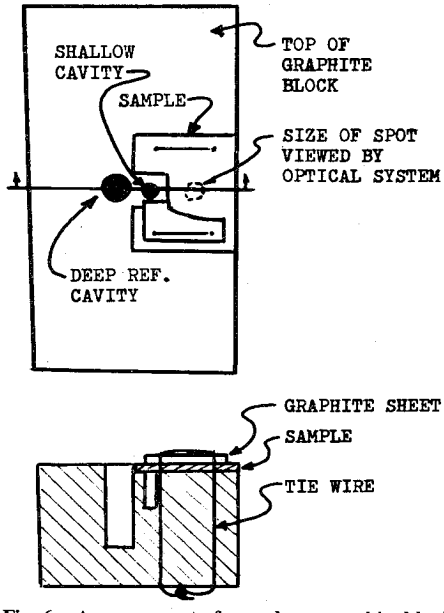

Fig. 6 Arrangement of sample on graphite block.

to measure this temperature difference. another thin sheet of graphite was attached to the top of the sample as shown. The sample sheet and the graphite sheet were tied down with tungsten wire.

Temperature and Energy Measurement

The emittance of a sample is determined by measuring the ratio of the intensity of radiation emitted from the sample to that emitted from the reference cavity. The intensity ratio is obtained from the ratio of the intensity factors (Fig. 4) corresponding to the null currents measured with the optical system viewing the sample and cavity. The sample emittance (ϵ_s) is calculated from the relation

$$\epsilon_s = \bar{g}\tau R \tag{1}$$

where $\bar{g}$ = the average effective emittance of the portion of the reference cavity being viewed by the optical system, τ = the ratio of the intensity factors corresponding to the reference lamp null currents obtained when viewing the sample and reference cavity, and R = the correction factor for sample-reference temperature difference as follows:

$$R = \frac{\exp(C_2/\lambda(T-\Delta T)) - 1}{\exp(C_2/\lambda T) - 1} \tag{2}$$

In Eq. (2), T = the temperature of reference cavity, ΔT = the temperature difference between reference cavity and sample, λ = the wavelength, and C_2 = the radiation constant in Planck's radiation equation.

The reference cavity is a hole approximately 5 mm in diam. and 25 mm deep. The effective emittance $\bar{g}$ was calculated by solving a set of integral equations, giving the radiosity distribution over the interior of a cylindrical enclosure. The basic method is described by Love.[5] The calculated emittance of the cavity was based on the temperature of the top surface of the block. This temperature is T in Eq. (2).

The existence of small temperature gradients can have a large effect on the value of ϵ_s. At 1800°K, the bottom of the reference cavity was 35°K hotter than the top surface. The calculated emittance of the cavity ($\bar{g}$) is 0.997 without the temperature gradient, but rises to 1.048 when it is included. A sample reference temperature difference (ΔT) of 1% of the reference temperature (T) can change the value of R by almost 10% at some wavelengths. Although the value of T has relatively little influence on the measurement, the temperature

differences must be measured to within 0.1 or 0.2% of the reference temperature.

Measurement of the temperature variations was accomplished with an optical pyrometer. Under ideal conditions, these devices can measure the temperature of a blackbody to within 0.1%. These measurements are influenced by such things as surface emittance, reflected radiation, and absorption of radiation by the media between the source and the instrument. If these factors remain constant, it is possible to measure a temperature diffence accurately, even though the absolute temperature measurement is in error.

As an example, assume that the surface of the block in Fig. 6 is at 1600°K and the surface of the top graphite sheet is at 1500°K. If the effective emittance of the graphite is 0.85 and the optical components absorb 5% of the emitted radiation, an optical pyrometer would give the following results. The top of the block would measure 1575°K; the graphite sheet would measure 1478°K;the measured difference is 98°K, whereas the true difference is 100°K. The pyrometer used (Leeds and Northrup Model 8642 Automatic) is capable of this order of resolution. An experienced observer with a visual pyrometer also can achieve good results.

By scanning the top surface of the block with the pyrometer, no significant temperature variations in the horizontal direction were observed. By sighting into the deep cavity and then into the shallow cavity, the vertical temperature gradient in the block could be determined. The field of view of the pyrometer was limited to a spot approximately 1½mm in diam. The shallow cavity was 2½mm in diam. by 12½mm deep, so that the pyrometer was able to focus onto the bottoms of the two cavities. The vertical gradient was found to be approximately linear, and varied from 10 to 60 deg./in. as the furnace temperature ranged from 1600° to 2400°K. The linear temperature gradient was used to determine the effective cavity emittance.

The sample-reference temperature difference (ΔT) was measured by sighting on the block and then on the top of the graphite sheet. It was assumed that the temperature drops occurred only at the contact surfaces between the graphite and sample sheets. Measured ΔT values are given in the results tables.

Sources of Error

Spectrometer

The accuracy of the spectrometer is influenced by three major factors. The calibration of the monochromator, electrical noise that interferes with the determination of the null point, and the calibration of the reference lamp. Monochromator calibration and performance specifications can be established to within the limits required for emittance measurement by following the manufacturer's instruction manual. The major source of electrical noise was the furnace power supply. It was reduced to an acceptable level with filters, which rejected the 60-Hz component. The reference lamp was used to measure the intensity ratio of two unknown sources. The acccuracy is determined by the accuracy of the sector disks, which are used to establish the calibration curves (Fig. 4). This was determined by dimensional measurement to be within $\pm 1/2\%$. Lamp stability was found to be a problem only when trying to operate with the glass envelope removed. For this reason the glass was not removed, since most of the measurements to be made were at wavelengths below 3 microns where the glass would not interfere. The systematic error associated with the spectometer was reduced to within $\pm 1\%$ without too much difficulty.

Sample and Reference Cavity

Temperature gradients in the sample-reference system were the greatest potential source of systematic error. These were corrected by the method described earlier within the limits of uncertainty of the ΔT measurements. Another possible source of error which could not be measured and corrected was that caused by stray radiation from the furnace hot zone being reflected from the sample surface into the optical system. Most of this radiation came from the heat shields covering the top of the hot zone.

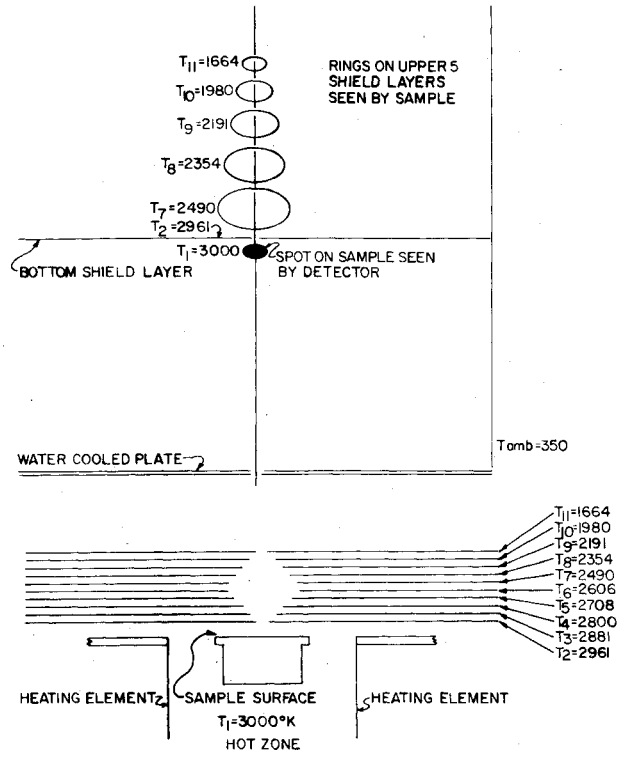

Fig. 7 Configuration of the apertures in the upper heat shields.

Figure 7 illustrates the arrangement of the heat shields at the top of the hot zone. The sample is located directly underneath a circular aperture in the bottom layer of the shield assembly. This layer gets almost as hot as the sample itself. Each successive layer gets cooler, as shown in Fig. 7 but each one emits radiation that could strike the sample and be reflected in the normal direction.

In order to reduce the amount of radiation reaching the sample, the apertures in the shield layers were recessed as shown, so that the sample receives direct radiation only from the bottom layer and the cooler top layers. Specular reflections from the sample could not be seen by the optical system. Diffuse reflections, however, will be measured, along with the emitted radiation, and make the measured value too high. An accurate analysis of these reflections cannot be performed without reflectivity data on the surfaces involved. In order to get an order-of-magnitude estimate of the amount of error which could be expected, a lumped system approximation [5] was performed on the surfaces that were in direct view of the sample shown in Fig. 7. This analysis indicated that the emittance of a sample with a diffuser reflectance of 0.2 would be biased high by 0.015. Samples with higher values of diffuse reflectance could be biased high by 2% or more.

In order to judge which sample may fall into this category, the specular component of reflectance of each sample was measured. The reflectometer used was a simple device normally used for checking the finish of polished metals. The measurement obtained from this instrument corresponds approximately to the specular reflectance as described by Love[5]. The spectral response of the detector was limited to visible wavelenghts. This measurement, although not extremely accurate, could be used qualitatively to judge whether a sample might have a high enough diffuse reflectance to present a problem with the emittance measurement. For example, the specular reflectance of a tungsten sample measured 0.38.

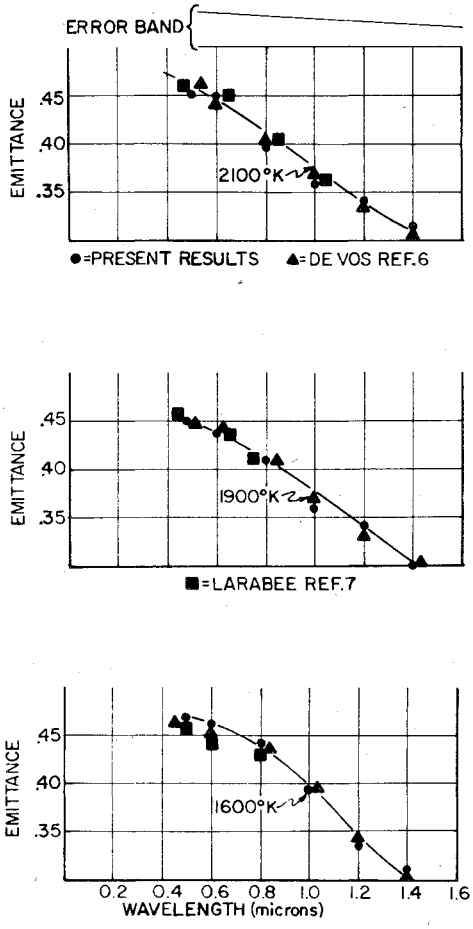

Fig. 8 Normal spectral emittance of tungsten.

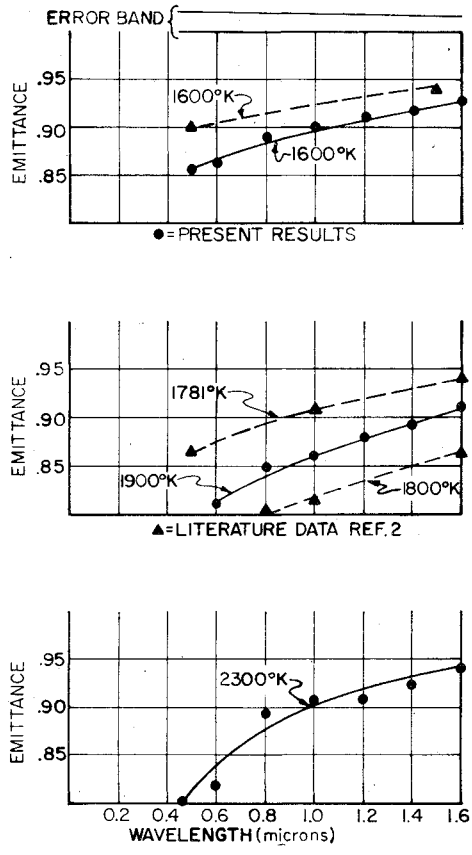

Fig. 9 Normal spectral emittance of graphite ATJ.

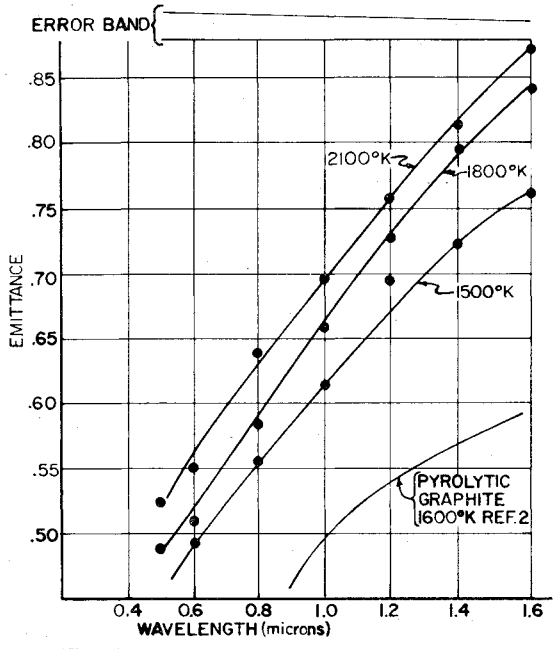

Fig. 10 Normal spectral emittance of carbon foam.

Since the emittance of the sample was approximately 0.45 at visible wavelengths, this leaves a value of 0.17 for the diffuse reflectance.

Random Error

The random error in the emittance measurements was estimated by statistical analysis of measurement data. Three separate measurements were required to determine the emittance of a sample. The quantity τ in Eq. (1) is the measured value of the sample-reference intensity ratio. The reference cavity emittance $\bar{g}$ is calculated from the cavity geometry and from the measured value of the vertical temperature gradient in the block. The quantity R is calculated from the measured value of the sample-reference temperature difference ΔT.

The standard deviation (σ) for each measured quantity was calculated from repeated measurements of the same value. The standard deviations for each of the three quantities in Eq. (1) then were calculated and combined to obtain the overall standard deviation for the emittance measurement:

$$\sigma\epsilon = \left\{\left[\frac{\partial \epsilon_s}{\partial \bar{g}}\sigma_g\right]^2 + \left[\frac{\partial \epsilon_s}{\partial \tau}\sigma_\tau\right]^2 + \left[\frac{\partial \epsilon_s}{\partial R}\sigma_R\right]^2\right\}^{1/2} \quad (3)$$

The magnitude of $\sigma\epsilon$ generally ranged from 0.01 to 0.02; it is shown on the emittance-vs-wavelength graphs as the width of the error band.

Results of System Operation

Tungsten

The tungsten samples were prepared from commercial grade tungsten sheets, ranging in thickness from 0.006 in. to 0.015 in. Profilometer measurements indicated a surface finish of 2 or 3 μ in. The reflectometer measurements gave values of 0.35 to 0.40 for the specular reflectance. The samples were wired down to the graphite reference block as described previously (see Fig. 6). The sample surface was cleaned with alcohol before installation in the furnace.

All measurements were made with a furnace pressure of approximately 5.0×10^{-5} Torr. The samples tested were subjected to temperatures between 1500° and 2300°K for a period of about 20 hr. while measurements were being made. The results of the before and after heating spectrographic analysis

are given in Table 1. The results of the measurements are given in Table 2 and plotted in Fig. 8.

Graphite ATJ

The reference cavity block (Fig. 7) was machined from commercial grade ATJ graphite supplied by Union Carbide Company. The top surface of the block was used as the sample surface. The surface finish measured approximately 30 μin. and there was no measurable component of specular reflection. The furnace pressure during operation remained around 5.0×10^{-5} torr. Some of the data are plotted in Fig. 9, along with the best available literature data for comparison. The literature data, taken from Touloukian,[2] is for siliconized ATJ of unspecified surface roughness. Most of the emittance data given for the different graphites fall in the 0.75

Table 1 Trace impurities of tungsten samples from spectrographic analysis.

Element	Before Heating	After Heating
Cr	40 PPM	40 PPM
Sb	20	30
V	20	30
Bi	10	10
Cs	200	100
Rb	100	100
Cu	2	10
Mo	60	60
Th	100	100
Ca	10	10
Fe	60	40
Na	20	20
Pb	10	10
Si	6	6
B	10	10
Sn	10	10
Zr	20	20
Co	10	10
U	100	100
WC	0	0

Table 3 Trace impurities of graphite ATJ from spectrographic analysis

Element	Before Heating	After Heating
Ag	1 PPM	1 PPM
Be	1	1
Cr	1	2000
Hf	10	10
Mg	10	10
Sb	1	1
Ta	100	5000
V	10	10
Al	10	10
Bi	10	10
Cs	60	60
Hg	10	10
Mn	1	20
Sc	1	1
W	10	5000
As	10	10
Cu	10	15
Mo	1	2500
P	100	100
Th	4	4
U	40	40
Ca	125	10
Fe	115	5000
Ir	2	2
Na	25	20
Pb	1	1
Si	180	40
Ti	10	600
Zn	60	60
B	5	1
K	20	20
Nb	1	200
Pd	6	6
Zr	2	200
Ba	15	1
Co	20	20
Li	10	10
Ni	4	100

Table 2 Measurement results for tungsten

λ Microns	τ	$g(\lambda)$	ΔT Deg C	$R(\lambda)$	Sample (Present)	Emittance (DeVos[6])	Sample Temperature Deg K
.5	.32	1.103	25	1.331	.470	.469	1600
.6	.34	1.084	25	1.269	.468	.456	1600
.8	.35	1.056	25	1.196	.442	.430	1600
1.0	.32	1.043	25	1.154	.385	.390	1600
1.2	.29	1.034	25	1.127	.338	.344	1600
1.4	.27	1.025	25	1.108	.307	.301	1600
1.6	.25	1.022	25	1.094	.380	.264	1600
.5	.32	1.121	28	1.254	.450	.463	1900
.6	.33	1.099	28	1.208	.438	.448	1900
.8	.34	1.069	28	1.152	.419	.421	1900
1.0	.31	1.053	28	1.120	.366	.381	1900
1.2	.30	1.043	28	1.099	.344	.340	1900
1.4	.26	1.033	28	1.085	.291	.304	1900
1.6	.25	1.029	28	1.074	.276	.270	1900
.5	.32	1.152	32	1.235	.455	.460	2100
.6	.32	1.118	32	1.192	.450	.446	2100
.8	.32	1.082	32	1.141	.396	.414	2100
1.0	.305	1.064	32	1.111	.361	.376	2100
1.2	.30	1.049	32	1.092	.343	.340	2100
1.4	.28	1.043	32	1.079	.315	.306	2100
1.6	.265	1.036	32	1.069	.293	.280	2100

Table 4 Measurement results for graphite ATJ

λ Microns	τ	g(λ)	ΔT Deg C	R(λ)	Sample Emittance	Sample Temperature, Deg K
.5	.77	1.100	0	1.00	.847	1600
.6	.79	1.085	0	1.00	.857	1600
.8	.84	1.068	0	1.00	.889	1600
1.0	.86	1.052	0	1.00	.899	1600
1.2	.88	1.040	0	1.00	.911	1600
1.4	.90	1.033	0	1.00	.925	1600
1.6	.92	1.028	0	1.00	.942	1600
.5	.695	1.120	0	1.00	.778	1900
.6	.745	1.096	0	1.00	.817	1900
.8	.80	1.068	0	1.00	.854	1900
1.0	.825	1.052	0	1.00	.868	1900
1.2	.85	1.040	0	1.00	.884	1900
1.4	.86	1.033	0	1.00	.888	1900
1.6	.90	1.028	0	1.00	.925	1900
.5	.675	1.180	0	1.00	.797	2300
.6	.715	1.146	0	1.00	.820	2300
.8	.81	1.106	0	1.00	.896	2300
1.0	.845	1.082	0	1.00	.914	2300
1.2	.86	1.064	0	1.00	.913	2300
1.4	.88	1.055	0	1.00	.928	2300
1.6	.89	1.047	0	1.00	.932	2300

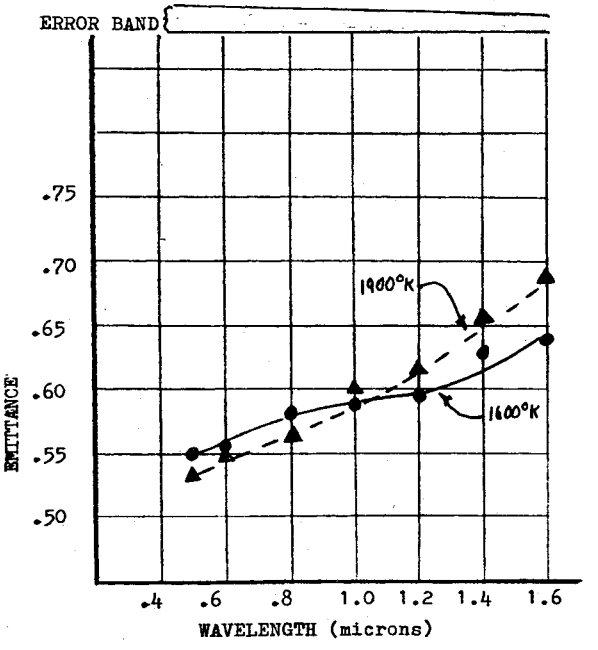

Fig. 11 Normal spectral emittance of aluminum oxide.

to 0.925 range, depending on composition, surface finish, and temperature. The results of the before-heating and after-heating spectrographic analyses are given in Table 3. The results of the measurements are given in Table 4.

Carbon Foam

The foam samples were cut into rectangular sheets, approximately 1/16 in. thick, and fastened to the reference block as shown in Fig. 6. The furnace pressure during measurement was 5.0×10^{-5} Torr. The complete spectrographic analysis is not presented, since the only significant change before and after heating was an increase in the tungsten content, from less than 10 ppm to approximately 1000 ppm. No significant changes in emittance were noted at lower temperatures after heating to 2100°K. Measurement results are given in Fig. 10. No literature data were available for carbon foam, however, the results appear to follow somewhat the emittance of some of the pyrolytic foams of carbon.

Table 5 Trace impurities of aluminum oxide sample spectrographic analysis

Element	Before Heating	After Heating
Ag	1 PPM	1 PPM
Be	1	3
Cr	70	50
Hf	30	30
Mg	1000	700
Sb	10	10
Ta	100	100
V	30	30
Bi	10	10
Cs	300	300
Mn	10	3
Rb	100	100
W	70	70
Cu	200	10
Mg	10	10
Au	3	3
Ca	2000	2000
Fe	1000	600
Na	3000	100
Pb	30	100
Si	900	10,000
Ti	3000	3000
Zr	100	100
K	3000	300
Nb	500	30
Pd	10	10
Sn	10	10
Zr	100	100
Ba	300	300
Co	10	10
Li	100	10
Ni	10	10

Table 6 Measurement results for aluminum oxide

λ Microns	τ	$\bar{g}(\lambda)$	ΔT Deg C	$\underline{R}(\lambda)$	Sample Emittance	Sample Temperature Deg K
.5	.385	1.103	22.5	1.294	.550	1600
.6	.415	1.084	22.5	1.240	.558	1600
.8	.48	1.049	22.5	1.154	.581	1600
1.0	.49	1.043	22.5	1.138	.582	1600
1.2	.51	1.034	22.5	1.114	.587	1600
1.4	.56	1.025	22.5	1.097	.630	1600
1.6	.58	1.022	22.5	1.084	.643	1600
.5	.375	1.121	31	1.284	.540	1900
.6	.41	1.099	31	1.232	.555	1900
.8	.45	1.069	31	1.169	.562	1900
1.0	.50	1.053	31	1.133	.600	1900
1.2	.54	1.043	31	1.110	.625	1900
1.4	.58	1.033	31	1.094	.655	1900
1.6	.62	1.029	31	1.082	.690	1900

Aluminum Oxide

These samples were cut from a block of high purity alumina supplied by a furnace manufacturer. They were approximately 1/16 in. thick, and had a surface finish of approximately 90 μin. Tables 5 and 6 and Fig. 11 give the measurement results. Because of a leak in the furnace, the pressure during measurement rose to approximately 1×10^{-3} Torr. Table 5 shows that the samples increased greatly in silicon content during heating. The silicon probably came from a vacuum grease, which was applied to several "O"-ring seals in an effort to stop the leak that developed.

References

[1]Gubareff, G. G., *Thermal Radiation Properties Survey*, Honeywell Research Center, 1960.

[2]Touloukian, Y. S., *Thermophysical Properties of High Temperature Solid Materials*, Thermophysical Properties Research Center, Purdue University, 1967.

[3]Blau, H. and Fischer, H., *Radiative Transfer from Solid Materials*, Macmillan, New York, 1962.

[4]Thorn, R. J. and Winslow, G. H., "Radiation of Thermal Energy from Real Bodies," *Temperature, Its Measurement and Control in Science and Industry*, Pt. 1, 1962, pp. 421-447.

[5]Love, T. J., *Radiative Heat Transfer*, Merrill Publishing, Columbus, Ohio, 1968, pp. 44, 61, 80–94.

[6]DeVos J. C., "A New Determination of the Emissivity of Tungsten Ribbon," *Physica*, Vol. 20, 1954, p. 690.

[7]Larrabee, R. D., "Spectral Emissivity of Tungsten," *Journal of the Optical Society of America*, Vol. 39, 1959, pp. 619–625.